

ARTICLES

Estimation of Effective Diameters for Molecular Fluids

Dor Ben-Amotz[†] and Dudley R. Herschbach^{*‡}

Corporate Research Science Laboratories, Exxon Research and Engineering Company, Annandale, New Jersey 08801 (Received: September 21, 1989)

Effective diameters of atoms and molecules can typically be estimated within about 1% from equation-of-state or compressibility data. These estimates correlate well with critical volumes, with molar refractivities, and with tabulated van der Waals volume increments. The correlations hold well even for markedly aspherical or polar molecules. Comparison of a simple perturbed hard-sphere equation of state (the Carnahan-Starling-van der Waals equation, denoted CS-vdW) with molecular dynamics simulations shows that surprisingly good values for both the Lennard-Jones radius and well depth (typically within 1% for σ_{LJ} , 10% for ϵ_{LJ}) can be obtained by using pressure-density isotherms or equivalent data. Together with empirical correlations, this permits the LJ potential parameters to be estimated simply from the density (at atmospheric pressure) and the heat of vaporization or boiling point temperature. The temperature dependence of the effective diameter can be estimated from a simple model originally introduced by Boltzmann. More sophisticated perturbative theories of liquids predict a small additional density dependence of the effective diameter. Simple analytical expressions for these theoretical models are presented. In particular, the CS-vdW equation is found to predict reliable absolute densities (within 1%) for liquids at high pressures where direct measurements become difficult.

I. Introduction

Many aspects of the modern theory of fluids affirm the venerable view of van der Waals, which contrasted the roles of repulsive and attractive forces.¹⁻⁵ In dense fluids, repulsive hard spheres offer a good zeroth-order model for the major excluded-volume and packing effects. The attractive forces provide a practically uniform cohesive background and have little influence on the fluid structure or dynamics. Current perturbation treatments of dense fluids thus take hard spheres as an appealing and tractable first approximation but use an effective diameter dependent on temperature and density to account for the softness of the repulsive potential. However, in various treatments the criteria used to define the effective hard-sphere diameter differ appreciably. Likewise, many semiempirical analyses⁶⁻¹² of fluid properties yield different effective diameters, as illustrated in Figure 1. Here we examine several of these diameters as functions of T and ρ and evaluate empirical correlations which provide practical approximations for their magnitude, temperature, and pressure dependence.

In section II we compare various empirical and theoretical measures of effective molecular diameters. We find that good estimates can be obtained simply from equation-of-state data. The corresponding molecular volumes correlate very well with molar refractivities and with both space-filling molecular volumes and critical volumes. In sections III and IV we consider the temperature and density dependence of the effective diameters and obtain estimates for molecules with interaction potentials resembling the Lennard-Jones potential. In section V we summarize practical estimation methods for both effective diameters and for the Lennard-Jones radius and well depth, tabulate parameters for 50 molecules, and discuss some applications.

II. Effective Hard-Sphere Diameters and Volumes

Experimental values of effective molecular diameters currently come mostly from second virial coefficients, diffusion or viscosity coefficients, or cross sections for molecular collisions.¹³ Such data

are often lacking. Equation-of-state data and molar refractivities are much more abundant. We find both offer simple, broadly applicable means to determine effective molecular diameters σ , and the results obtained prove remarkably concordant with values from other sources.

A. Diameters from CS-vdW Equation of State. The excluded-volume parameter in the van der Waals equation provided early estimates of molecular size. We employ this same method with a modified version of the equation, designated as CS-vdW. This relates the compressibility factor $Z = P/\rho k_B T$ to the hard-sphere packing fraction $\eta = (\pi/6)\rho\sigma^3$ via

$$Z_{CS-vdW} = (1 + \eta + \eta^2 - \eta^3)(1 - \eta)^{-3} - 4(\tau/T)\eta \quad (1)$$

The first term represents the excluded-volume effect by the Carnahan-Starling formula,¹⁴ which closely approximates the seven known virial coefficients and the hard-sphere equation of state found in Monte Carlo computer simulations. The second term is the attractive portion of the original van der Waals equation, characterized by a parameter τ , proportional to the Boyle temperature. Several variants of eq 1 have been examined previously, with either or both of σ and τ taken as constant or as parametrized functions of T or ρ or both.¹⁵⁻²¹ These previous

- (1) Zwanzig, R. W. *J. Chem. Phys.* **1954**, *22*, 1420.
- (2) Barker, J. A.; Henderson, D. *Rev. Mod. Phys.* **1976**, *48*, 587.
- (3) Andersen, H. C.; Chandler, D.; Weeks, J. D. *Adv. Chem. Phys.* **1976**, *34*, 105.
- (4) Chandler, D.; Weeks, J. D.; Andersen, H. C. *Science* **1983**, *220*, 787.
- (5) Hansen, J. P.; McDonald, I. R. *Theory of Simple Liquids*, 2nd ed.; Academic Press: New York, 1986, and work cited therein.
- (6) Mourits, F. H.; Rummens, F. H. A. *Can. J. Phys.* **1977**, *55*, 3007.
- (7) De Ligny, C. L.; van der Veen, N. G. *Chem. Eng. Sci.* **1972**, *27*, 391.
- (8) Wilhelm, E. *J. Chem. Phys.* **1973**, *58*, 3558.
- (9) Mayer, S. W. *J. Phys. Chem.* **1963**, *67*, 2160.
- (10) Ertl, H.; Dullien, F. A. L. *AIChE J.* **1973**, *19*, 1215.
- (11) Tanabe, K.; Hiraishi, J. *Mol. Phys.* **1980**, *39*, 1507.
- (12) Bondi, A. *J. Phys. Chem.* **1964**, *68*, 441.
- (13) Hirschfelder, J. O.; Curtiss, C. F.; Bird, R. B. *Molecular Theory of Gases and Liquids*; Wiley: New York, 1954.
- (14) Carnahan, N. F.; Starling, K. E. *J. Chem. Phys.* **1969**, *51*, 635.
- (15) Longuet-Higgins, H. C.; Widom, B. *Mol. Phys.* **1964**, *8*, 549.
- (16) Vera, J. H.; Prausnitz, J. M. *Chem. Eng. J. (Laussane)* **1972**, *3*, 1.
- (17) Carnahan, N. F.; Starling, K. E. *AIChE J.* **1972**, *18*, 1184.
- (18) Gubbins, K. E. *AIChE J.* **1973**, *19*, 684.

[†] Present address: Department of Chemistry, Purdue University, West Lafayette, IN 47907.

[‡] Exxon Faculty Fellow from Harvard University, Department of Chemistry, 12 Oxford Street, Cambridge, MA 02138.

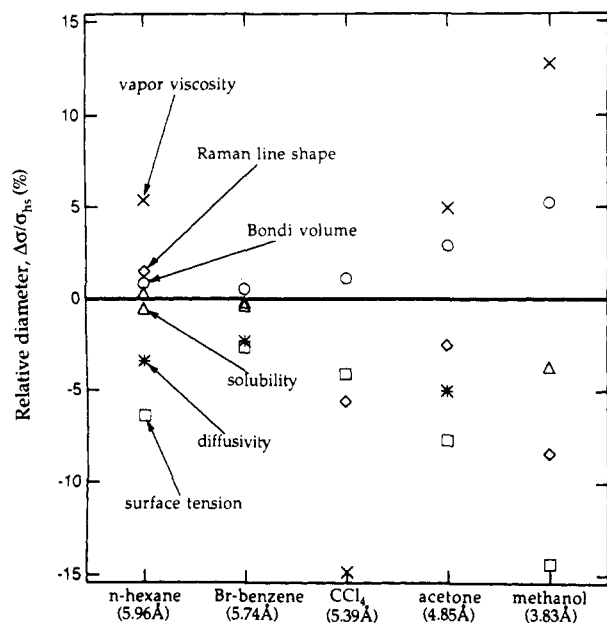


Figure 1. Comparison of effective hard-sphere diameters obtained from various experimental data, for five typical molecules. Ordinate shows percentage deviation from σ_{hs} derived from CS-vdW equation of state, eq 1. Values of σ_{hs} (in Å units, at 20 °C) shown along abscissa. Points pertain to gas viscosity⁶ (crosses), liquid diffusion coefficient⁷ (asterisks), liquid surface tension⁸ (squares), solubility^{9,10} (triangles), Raman line shapes¹¹ (diamonds), and space-filling volumes from Bondi tabulation¹² (circles).

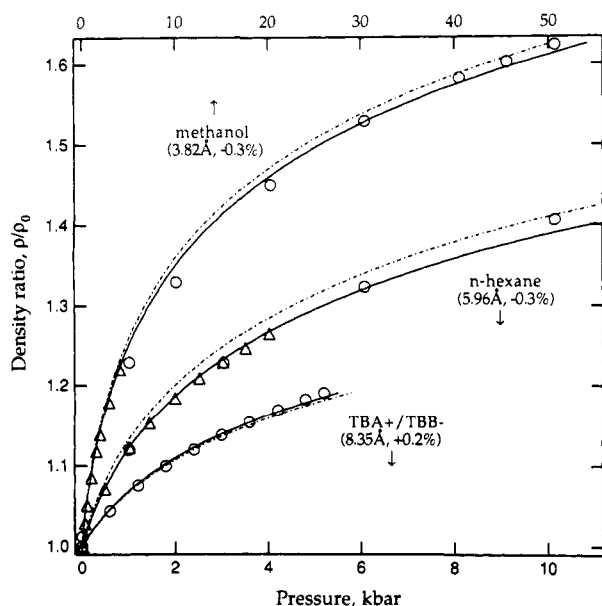


Figure 2. Comparison of experimental pressure-density isotherms (points, data from refs 22–24) with CS-vdW equation of state, eq 1. Reference density ρ_0 pertains to atmospheric pressure. Temperature is 25 °C for methanol and *n*-hexane and 140 °C for the molten organic salt tetrabutylammonium/tetrabutylborate. Parameters σ and τ fit either to (a) high-pressure data (full curves) or to (b) density and compressibility at atmospheric pressure (dashed curves). Values of σ for (a) case are indicated as well as percent change of σ for the (b) case.

applications have dealt almost solely with data for the region of low Z (<1), however, where eq 1 provides only a rough approximation. We find that for high Z it becomes much more satisfactory. In this region, the σ values fitted to data are sharply

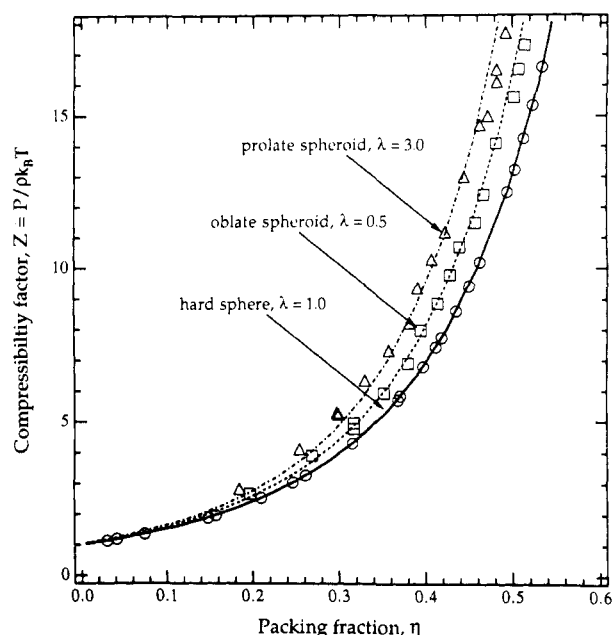


Figure 3. Effect of shape on equation of state of hard-body fluids. Points from Monte Carlo computations²⁵ for spheres ($\lambda = 1.0$, circles), oblate spheroids ($\lambda = 0.5$, squares), and prolate spheroids ($\lambda = 3.0$, triangles). Curves show the Carnahan-Starling equation of state, the first term of eq 1, with the effective diameter chosen to make the hard-sphere volume equal to that for the Monte Carlo calculation in the sphere case (full curve), 1.02 times the volume of the oblate spheroid (dotted curve), and 1.04 times the volume of the prolate spheroid (dot-dashed curve).

determined and insensitive to alternative choices of input or to substantial adjustments in the τ parameter. Figure 2 illustrates this happy circumstance for three substances of markedly different chemical character.^{22–24}

The σ values are also insensitive to substantial deviations of the molecular shape from sphericity. Figure 3 illustrates this with equation-of-state data obtained from Monte Carlo computations of hard spheres, oblate spheroids, and prolate spheroids.²⁵ We find that eq 1 yields good agreement with these data if the hard-sphere volume, $V_{hs} = (\pi/6)\sigma^3$, is adjusted to be slightly larger than the spheroid volume (2% larger for oblate case, 4% for prolate). Thus, a change of $\sim 1\%$ in the magnitude of the effective diameter will take account of such shape effects.

At a given temperature, the parameters σ and τ can be determined to good accuracy from several kinds of data; the options are outlined in section V. Particularly welcome is the result that satisfactory parameters can be obtained solely from data pertaining to atmospheric pressure.

B. Molecular Size from Molar Refraction. Another early means for estimating effective diameters, long considered outmoded, employed measurements of the refractive index n to derive values of the molecular polarizability.²⁶ This serves as a measure of the volume, which is evaluated from

$$V_n = [(n^2 - 1)/(n^2 + 2)]/\rho \quad (2)$$

with ρ the number density. Strictly the refractive index should pertain to long wavelengths, but values for visible light are adequate. The data required for eq 2 are plentiful. Although V_n actually pertains to an effective electron density rather than a geometric volume, and the values obtained are substantially smaller

(19) Oelrich, L. R.; Knapp, H.; Prausnitz, J. M. *Fluid Phase Equilib.* **1978**, *2*, 163.

(20) Johnston, K. P.; Eckhart, C. A. *AIChE J.* **1981**, *27*, 773.

(21) Cotterman, R. L.; Schwartz, B. J.; Prausnitz, J. M. *AIChE J.* **1986**, *32*, 1787.

(22) Kubota, H.; Tsuda, S.; Murata, M.; Yamamoto, T.; Tanaka, Y.; Makita, T. *Rev. Phys. Chem. Jpn.* **1979**, *49*, 59. Isdale, J. D.; Eastal, A. J.; Woolf, L. A. *Int. J. Thermophys.* **1985**, *5*, 439.

(23) Dymond, J. H.; Young, K. J.; Isdale, J. D. *Int. J. Thermophys.* **1980**, *1*, 345.

(24) Grindley, T. Ph.D. Thesis, Stanford University, 1971 (UMI No. 72-5920).

(25) Boublik, T.; Nezbeda, I. *Collect. Czech. Chem. Commun.* **1986**, *51*, 2301.

(26) Glasstone, S. *Physical Chemistry*, 2nd ed.; D. Van Nostrand: New York, 1954; p 542.

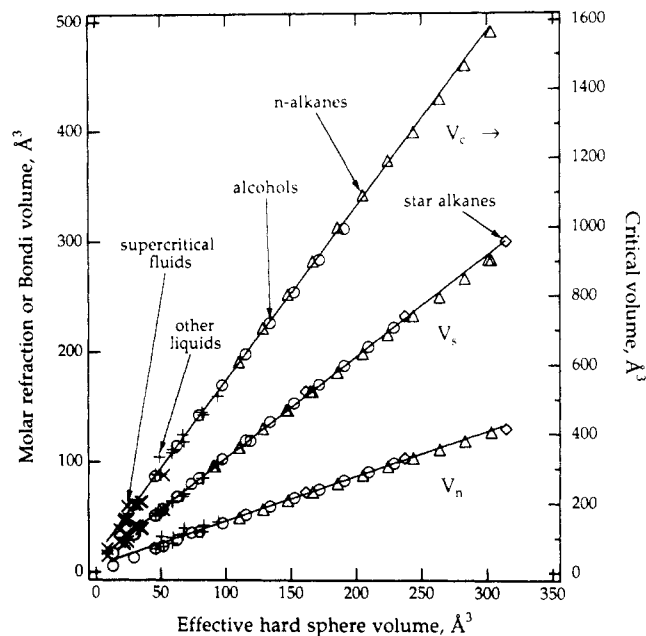


Figure 4. Correlation of hard-sphere volumes (abscissa scale) corresponding to diameters obtained from CS-vdW equation of state, eq 1, with three others: V_c , the critical volume (uppermost points, ordinate scale at right); V_n , derived via eq 2 from molar refractivity (lowermost points, ordinate at left); V_s , the space-filling volume derived from "van der Waals increments" tabulated by Bondi¹² (middle points, ordinate at left). Values of V_{hs} are obtained from fits to pressure-density isotherms at 20 °C (Table III). Linear correlations are given in Table I.

than those computed from the CS-vdW diameters, we find a remarkably good correlation between these two measures of molecular volume. Thus, the V_n values are quite useful in interpolating or extrapolating estimates of diameters, since the extensive refractive index data have been codified by rules that enable the polarizability to be approximated by summing contributions from constituent bonds and groups.²⁷

C. Correlation of Empirical Volume Estimates. Figure 4 shows how well the molecular volumes V_{hs} computed from the CS-vdW effective diameters correlate with three other measures of size: V_n from molar refractivity, V_c the critical volume,²⁸ and V_s the space-filling volume derived from "van der Waals increments" tabulated by Bondi.¹² The correlation with V_n is excellent for alkanes and alcohols but less good for halogenated molecules; apparently this reflects qualitative variations in electronic structure. The correlation with V_c is quantitatively very good, even though the critical volume is typically 5 times larger than the CS-vdW volume for a given molecule. If V_c is known, the σ for eq 1 can be predicted within about 1%. This holds for a wide variety of molecules, including long chain linear alkanes (up to C_{17}) as well as aromatics and the strongly associated alcohols and polyalcohols. The accuracy and scope of the correlation are gratifying, in view of the disparity in magnitude and the fact that the critical volumes pertain to a much more complicated regime of the equation of state where simple analytical equations such as eq 1 are not accurate. Likewise, the CS-vdW effective hard-sphere volumes also correlate well with the Bondi molecular space-filling volumes V_s , which are computed by simply summing tabulated increments for the various atoms and functional groups in the molecule. In this case the correlation can be used to predict the effective hard-sphere volumes within about 1% in the absence of any equation-of-state data. Furthermore, the hard-sphere volumes are remarkably similar in magnitude to the molecular space-filling volumes, typically within ~5%. This kinship is all the more striking because the space-filling volumes

(27) Weast, R. D., Ed. *Handbook of Chemistry and Physics*, 67th ed.; CRC Press: New York, 1986; p E-371.

(28) Landolt-Bornstein *Zahlenwerte und Funktionen*; Springer: Berlin, 1971; Vol. 2, Part 1.

TABLE I: Empirical Correlations

Effective Molecular Diameter and Volume^a

$$V_{hs} = (\pi/6)\sigma^3 \text{ or } \sigma = 1.244(V_{hs})^{1/3}$$

$$V_{hs} = 0.1973(V_c - 44.28)$$

$$= 1.086(V_s - 9.94)$$

$$= 2.473(V_n - 5.53)$$

Attractive Energy Density Parameter^b

$$\tau = 6.70(T_b - 39) = 4.77(T_c - 90)$$

$$= 1.30[(\Delta H_{vap}/R) - 101]$$

^a Molecular diameter in Å, volume in Å³. ^b Attractive parameter τ , boiling temperature T_b , or critical temperature T_c and heat of vaporization in kelvin.

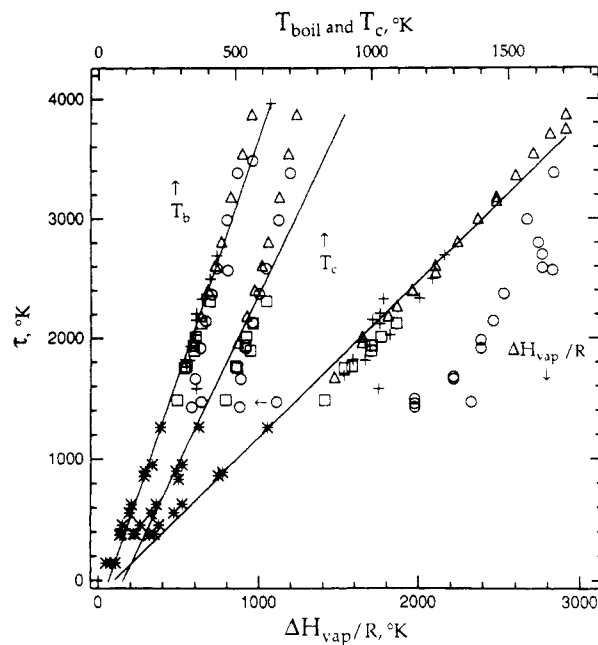


Figure 5. Correlation of attractive energy density parameter τ for CS-vdW equation of state, from eq 1, with heat of vaporization at the normal boiling point (1 atm), with boiling point temperature, and with critical temperature. Values of τ are obtained from fits to pressure-density isotherms at 20 °C (Table III); symbols designating different substances are the same as Figure 4, except for squares, which denote haloalkanes. Nominal linear correlations are given in Table I.

are not spherical but reflect the volumes of the bumpy molecular contours.

Table I provides numerical formulas for estimating the CS-vdW effective diameter and the corresponding volume V_{hs} from V_c , V_s , or V_n .

D. Attraction Correlated with Vaporization and Boiling Point.

A complementary correlation, of lesser accuracy and scope, has also been found for the τ parameter. Qualitatively, this parameter represents a binary interaction energy multiplied by the number of nearest neighbors. This is also roughly the interpretation of the heat of vaporization of a liquid. Indeed, as shown in Figure 5, we find that for many molecules the value of τ obtained from fitting eq 1 at 20 °C is quite similar in magnitude to $\Delta H_{vap}/R$ at the normal (1 atm) boiling point of the liquid. Substantial deviations from the correlation occur chiefly for associated liquids such as the alcohols. According to Trouton's rule,²⁹ ΔH_{vap} is approximately proportional to the boiling temperature T_b for simple liquids. Thus, τ should be roughly proportional to T_b also, and Figure 5 includes this convenient version of the correlation. There is also a correlation with the critical temperature T_c , but this deviates substantially from linearity. Table I includes the corresponding numerical formulas for estimating τ from these correlations.

E. Theoretical Variants of Effective Hard-Sphere Diameters.

The effective diameters introduced in perturbation theories for

(29) See, for example: Nash, L. J. *Chem. Educ.* **1984**, *61*, 981.

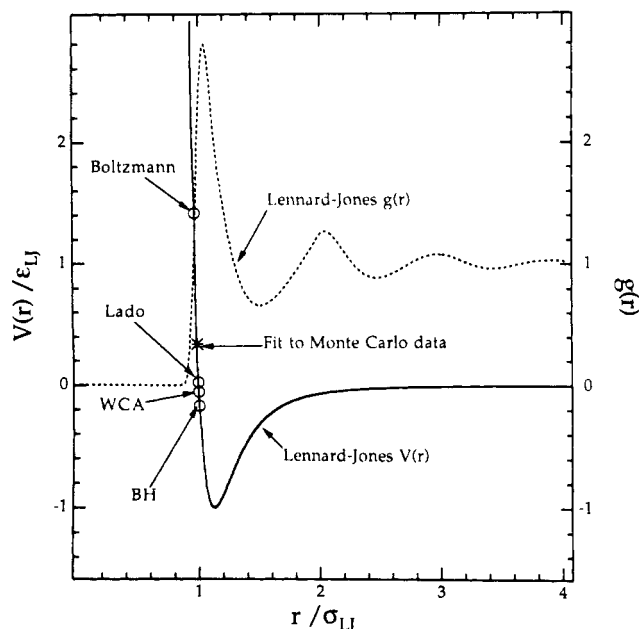


Figure 6. Effective hard-sphere diameters for Lennard-Jones (6,12) potential, according to various theoretical criteria, as specified in text. Points show location of the corresponding diameters (for a reduced temperature $T^* = k_B T / \epsilon_{LJ} = 1.25$) relative to the potential function and to the radial distribution function (for reduced density $\rho^* = \rho \sigma_{LJ}^3 = 0.85$ and $T^* = 1.27$). Asterisk indicates the diameter obtained by fitting data from computer simulation for a Lennard-Jones system to the CS-vdW equation.

dense fluids are specified with reference to an intermolecular potential function, usually the Lennard-Jones (6,12) potential. Figure 6 illustrates how the effective σ 's are related to this potential and to its radial distribution function for four different theoretical variants (at a particular reduced temperature and density). Simplest is a criterion suggested by Boltzmann, according to which the diameter is specified as the distance of closest approach, averaged over collisions that reach the repulsive wall of the potential.³⁰⁻³² Another simple criterion is employed in the Barker-Henderson (BH) perturbation treatment.² This involves integrating over the repulsive portion of the potential. A more complicated criterion for the effective diameter is used in the Weeks, Chandler, and Anderson (WCA) perturbation theory.^{3,4} This considers the repulsive and attractive forces (rather than the potential) and takes the cutoff at the zero-force point (potential minimum); a numerical integration over the radial distribution function of a trial hard-sphere fluid is required to obtain the diameter. Values are shown for the original version (WCA) and for a modification³³ (Lado) which improved consistency with thermodynamic criteria. All four theoretical models predict a significant temperature dependence of the diameter, but only the WCA and Lado models predict a density dependence.

Explicit expressions for computation of these various diameters for a Lennard-Jones potential are given in Table II; as described in Appendix A, these have been formulated to avoid need for any integrations or iterations.

III. Temperature Dependence of Effective Diameter

Previous experimental and theoretical estimates of the temperature variation of effective hard-sphere diameters are in the range $\partial\sigma/\partial T \approx -1 \times 10^{-4}$ to -5×10^{-4} Å/K, corresponding typically to a decrease of a few percent for an increase of 100 K. As shown in Figure 7, we find similar results. The four variant theoretical diameters considered (full curves) are compared with

TABLE II: Theoretical Effective Diameters^a

model	σ_0^*	T_0^*
BAS ^b	1.1225	0.500
BH ^c	1.1154	1.759
WCA ^d	1.1137	1.502
Lado ^d	1.1152	1.330
Monte Carlo ^e	1.1532	0.527

^a Parameters for eq 3 in reduced form: $\sigma_0^* = \sigma_0 / \sigma_{LJ}$, $T_0^* = k_B T_0 / \epsilon_{LJ}$. ^b Boltzmann-Andrews-Speedy, refs 30-32. ^c Barker-Henderson, ref 2, modified to take potential minimum as zero of energy. ^d Weeks-Chandler-Anderson, refs 3 and 4; Lado, ref 33. Values of T_0^* listed pertain to a reduced density ρ^* of unity; elsewhere (in range $0.2 < \rho^* < 1.1$) compute from $(T_0^*)^{-1/2} = 0.72157 + 0.04561x - 0.07468x^2 + 0.12344x^3$ for WCA and $(T_0^*)^{-1/2} = 0.73454 + 0.10250x - 0.12960x^2 + 0.15976x^3$ for Lado, with $x = \rho^* = \rho \sigma_{LJ}^3$, the reduced density. ^e Parameters derived by fitting CS-vdW formula to equation-of-state data from Monte Carlo simulations of ref 34.

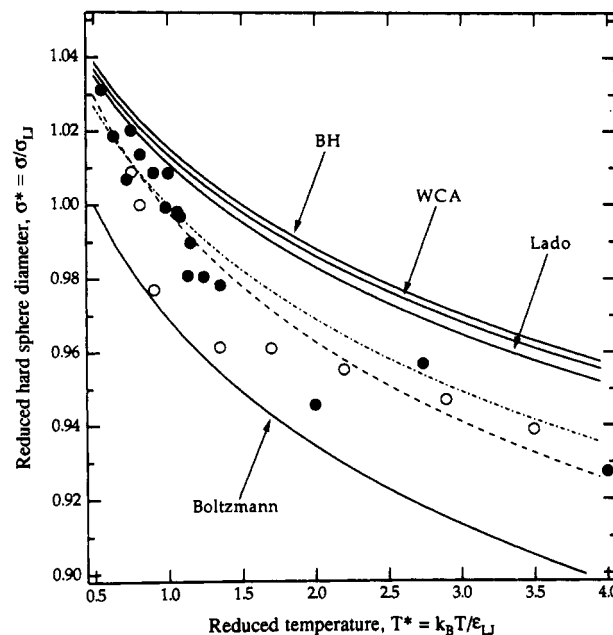


Figure 7. Effective hard-sphere diameters for Lennard-Jones potential as functions of reduced temperature, for theoretical models specified in text. Curves are obtained from formulas of Table II (with $\rho^* = 0.7$ for WCA and Lado models); solid and open points are from fitting CS-vdW equation to computer simulation and to experimental argon data, respectively.

results obtained from computer simulations (points) for a Lennard-Jones potential.³⁴ The temperature dependence in each case resembles the simple result, derived in Appendix A, for the Boltzmann diameter:

$$\sigma(T) = \sigma_0 [1 + (T/T_0)^{1/2}]^{-1/6} \quad (3)$$

where σ_0 and T_0 are parameters. For the Lennard-Jones potential, $\sigma_0^* = \sigma_0 / \sigma_{LJ} = 2^{1/6} = 1.1225$ and $T_0^* = 1/2$, in terms of the customary reduced units for temperature, $T^* = k_B T / \epsilon_{LJ}$. These parameter values pertain to an unadulterated Boltzmann model, as employed by Speedy.³² For the BH, WCA, and Lado models, likewise applied to the LJ potential, we find that eq 3 provides a close approximation with practically the same value for σ_0^* but different values for T_0^* , as listed in Table II. In the WCA and Lado variants, T_0^* also becomes a function of the reduced density, $\rho^* = \rho \sigma_{LJ}^3$, and decreases substantially ($\sim 20\%$) over the fluid range ($\rho^* = 0-1.1$).

The points included in Figure 7 were obtained by fitting the CS-vdW equation (as described in section V) to pressure-density isotherms evaluated by Monte Carlo computer simulations for the LJ (6,12) potential. The simulation data,³⁴ which span the

(30) Boltzmann, L. *Lectures on Gas Theory*; Brush, S., Translator; University of California Press: Berkeley, 1964; p 169.

(31) Andrews, F. C. *J. Chem. Phys.* **1976**, *64*, 1941, 1948.

(32) Speedy, R. J.; Prielmeier, F. X.; Vardag, T.; Lang, E. W.; Ludemann, H.-D. *Mol. Phys.* **1989**, *66*, 577.

(33) Lado, F. *Mol. Phys.* **1984**, *52*, 871.

(34) Nicolas, J. J.; Gubbins, K. E.; Streett, W. B.; Tildesley, D. J. *Mol. Phys.* **1979**, *37*, 1429.

range $0.5 < T^* < 4$, pertain to the dense fluid and liquid regimes. This use of the CS-vdW equation enabled us to correlate the effective hard-sphere diameter $\sigma(T)$ and the attractive parameter τ with the LJ diameter σ_{LJ} and well depth ϵ_{LJ} . Thereby, we can readily link up any correlations of σ or τ with thermodynamic properties to the molecular potential parameters. Again, we found that $\sigma(T)$ can be described quite satisfactorily by the Boltzmann form given in eq 3. This is illustrated by two curves shown in Figure 7. One curve (dot-dashed) corresponds to $\sigma_0^* = 1.1225$ and $T_0^* = 1$ and the other (dashed) to $\sigma_0^* = 1.1532$ and $T_0^* = 0.527$, as determined by a least-squares fit to the data. For a wide range of substances, the values of σ_{LJ} and ϵ_{LJ} derived (using the least-squares result) from the empirical σ and τ of the CS-vdW equation agree closely (as illustrated in section V) with other estimates of the Lennard-Jones parameters. Within the noise of the simulation data, we find the attractive parameter τ is just a constant; in reduced units

$$\tau^* = k_B \tau / \epsilon_{LJ} \approx 3.9 \pm 0.15 \quad (4)$$

This result permits us to estimate the well depth directly from the empirical τ value. Then we estimate σ_{LJ} from eq 3 using this ϵ_{LJ} and the σ from CS-vdW at the experimental temperature. Despite considerable uncertainty in the estimate of the well depth (typically 5–10%), this procedure usually yields good estimates for σ_{LJ} (typically within 1%), by virtue of the 1/6 root in eq 3, the Boltzmann formula.

When sufficiently extensive and accurate equation-of-state data are available, the CS-vdW analysis to determine $\sigma(T)$ may be extended by including in τ a mild temperature dependence, described by

$$\tau = \tau_0 [1 - (T_A/T)] \quad (5)$$

In Appendix B, the quantities τ_0 and T_A are related to T_B , the Boyle temperature. Typically, we find τ_0 is about 10–25% larger than T_B . If τ is taken as a constant, as in the original van der Waals equation, then $\tau = T_B$; however, our empirical result of eq 4 is 14% larger than $T^* = 3.42$, the reduced Boyle temperature for a LJ potential.¹³

IV. Pressure Dependence of Effective Diameter

Effective diameters vary much less with density than with temperature. This is evident from the limited empirical results available, as well as theoretical estimates. We have derived experimental estimates from data on the pressure dependence of the refractive index.³⁵ From eq 2 we find the corresponding molecular volumes V_n decrease roughly 0.2%/kbar with increase in pressure; typically, this amounts to a decrease in the diameter by $\partial\sigma/\partial P \approx -3 \times 10^{-3} \text{ \AA}/\text{kbar}$.

Figure 8 displays these volumes $V_n(P)$ for four molecules together with theoretical results computed for a Lennard-Jones potential. Of the theoretical variants considered in Figures 6 and 7, only the WCA and Lado diameters vary with density. These were evaluated by using parameters for argon ($\sigma_{LJ} = 3.4 \text{ \AA}$, $\epsilon_{LJ}/k_B = 120 \text{ K}$) in order to provide an absolute pressure scale for the theoretical curves. The upper abscissa gives the pressure in reduced LJ units, $P^* = P/P_{LJ}$, with $P_{LJ} = \epsilon_{LJ}/\sigma_{LJ}^3$.³ The theoretical curves can be used to estimate the pressure dependence for any LJ system, by merely rescaling the abscissa. For example, typical LJ parameters for a hexane-like molecule ($\sigma_{LJ} \approx 5.8 \text{ \AA}$, $\epsilon_{LJ}/k_B \approx 500 \text{ K}$) give $P_{LJ}(\text{hexane})/P_{LJ}(\text{argon}) \approx 0.38/0.455 = 0.84$; the pressure scale for hexane hence can be estimated by multiplying the lower abscissa by this factor or the upper abscissa by $P_{LJ}(\text{hexane})$. For a methanol-like molecule ($\sigma_{LJ} = 3.8 \text{ \AA}$, $\epsilon_{LJ}/k_B = 380 \text{ K}$), the corresponding factor is 2.25, and this ratio does not vary by more than about a factor of 2 for other typical molecules. The argon pressure scale thus serves as a rough approximation to the theoretical prediction for other molecules.

Figure 9 shows curves for the WCA and Lado effective diameters as functions of density, again in reduced LJ units. We obtained the points by numerical integrations^{33,36} and the full

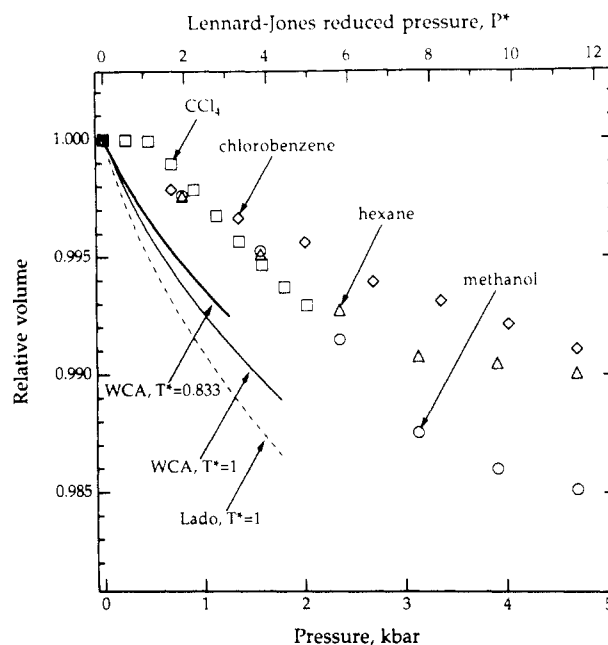


Figure 8. Pressure dependence for volumes V_n derived from molar refractivity data,³⁵ compared with calculations for Lennard-Jones potential according to WCA and Lado theoretical models, as described in text. The volumes obtained at $P = 0$ are 13.7, 44.1, 50.0, and 56.7 \AA^3 for methanol, carbon tetrachloride, hexane, and chlorobenzene, respectively. The model calculations pertain to a limited pressure range due to freezing of the LJ system, which occurs near $P^* = 1.9$ and 4.4 for $T^* = 0.833$ and 1.0, respectively.

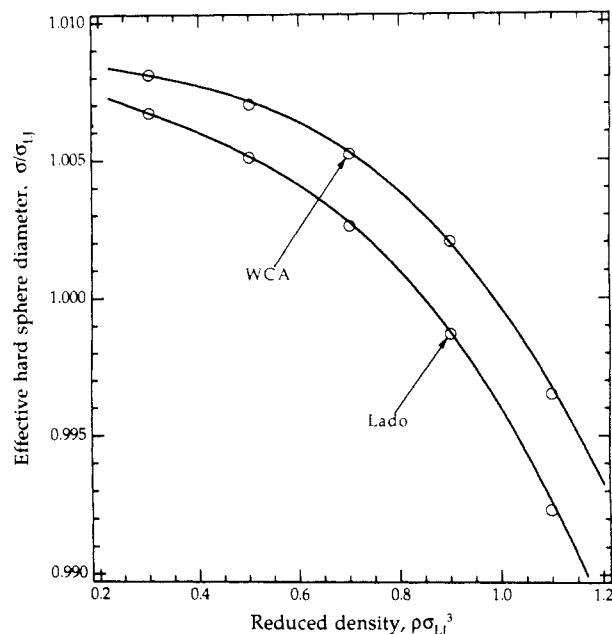


Figure 9. Density dependence of effective hard-sphere diameter for Lennard-Jones (6,12) potential at $T^* = 1.25$ according to WCA and Lado criteria. Curves are computed from formulas of Table II. Points obtained from numerical integrations using the Verlet-Weis approximation³⁶ for the hard-sphere cavity distribution function.

curves from the approximation formulas of Table II. The dependence on density is weak at low density and only becomes appreciable at high density, but there (in the liquid density regime) the density changes only slightly over a wide pressure range. Accordingly, in practice the experimental $V_n(P)$ curves usually do not correspond to an appreciable range of density, so that comparisons with the theoretical results are best made in terms of pressure rather than density.

(35) Vedam, K.; Limsuwan, P. *J. Chem. Phys.* **1978**, *69*, 4762.

(36) Verlet, L.; Weis, J.-J. *Phys. Rev. A* **1972**, *5*, 939.

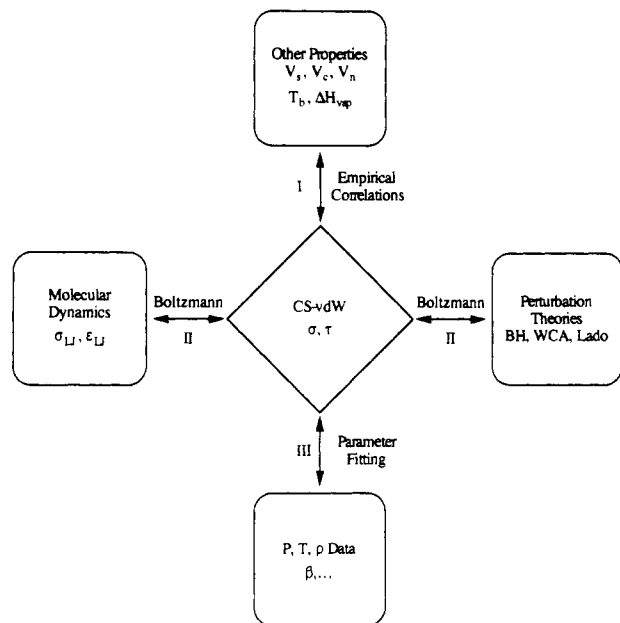


Figure 10. Schematic diagram showing how the CS-vdW equation is connected with equation-of-state data ("home base"), linked by parameter fitting, as in Figures 2 and 3 and Table III), other experimental properties ("second base", linked by empirical correlations of Figures 4 and 5 and Table I), as well as perturbation treatments ("first base", Figures 7 and 9) and the molecular dynamics simulations ("third base", Figure 7), both linked by the Boltzmann criterion (Table II).

The pressure dependence derived from the molar refractivity data is noticeably weaker than predicted by the WCA and Lado theoretical models. However, the rough agreement is probably more significant than the disparity, in view of the rather crude link between index of refraction and molecular volume and the substantial deviation of real fluids from the LJ potential. Thus, we estimate that for pressures up to about 10 kbar, which includes the typical liquid range, the effective diameter usually decreases by only 0.3% or less. This permits us to neglect the pressure or density dependence of the hard-sphere diameter when fitting the CS-vdW equation of state to data in this range.

V. Discussion

In summary, Figure 10 displays the overall scheme we have examined. The CS-vdW equation, augmented by the Boltzmann criterion and empirical correlations, serves as a four-pole switchbox connecting equation-of-state data with other experimental properties as well as with the perturbation treatments and the molecular dynamics simulations. Here we tabulate values of the σ and τ parameters derived from data for representative molecules, specify the options deemed most practical for estimating the magnitude and dependence on T and ρ of effective diameters, and illustrate some applications of this switchbox.

A. Evaluating the CS-vdW Equation of State. Table III gives results for 50 molecules obtained by fitting the CS-vdW form of eq 1 to pressure-density isotherms.^{28,37-52} The values listed

for σ and τ and their temperature derivatives pertain to 20 °C. Usually data spanning at least $P = 1\text{--}1000$ atm and $T = 10\text{--}30$ °C were used in evaluating these quantities. Rather than employing a nonlinear least-squares algorithm, we used a simpler procedure that was constrained to fit data for atmospheric pressure, the best known points. For each isotherm, this involved fitting σ and τ to a pair of experimental densities, at $P = 1$ atm and some higher pressure. An arbitrarily close fit is readily obtained by iterative guessing. A good first try for σ is usually close to $\rho^{-1/3}$; this guess is then used to evaluate a first estimate for τ by solving eq 1 at the lower density. With these trial values we compute the pressure at the higher density and adjust the parameters by Newton's method until a good fit is obtained to both data points. The procedure is then repeated for another high-pressure point. For all the substances examined (more than 75), the resulting parameters (σ , τ) obtained by using data for various points are invariably found to be very similar; thus, the best overall values were simply taken as the arithmetic mean. Typical results of such fits are shown in Figure 2.

Comparison of the parameters obtained for different isotherms showed σ^{-6} is accurately linear with $T^{1/2}$ and τ with T^{-1} , in accord with the simple approximations of eqs 3 and 5. Rather than tabulating the corresponding coefficients (σ_0 , T_0) and (τ_0 , T_A), however, we give instead in Table III the derivatives $T \partial\sigma/\partial T$ and $T \partial\tau/\partial T$. This was deemed more practical (in limited space). Otherwise, computations would be necessary even to obtain $\sigma(T)$ and $\tau(T)$ at the reference temperature ($T = 293$ K), whereas the derivatives are usually small enough to provide an easy estimate of the temperature correction for T not too different from the reference case. The actual coefficients (σ_0 , T_0) and τ_0 , T_A) are readily obtained from formulas given in Appendix C.

Several rules of thumb emerged from the parameter fitting for Table III and many other similar computations. For a given substance, the variation in σ values obtained by using equation-of-state data from different sources (including data at $P = 1$ atm as well as high pressures) is seldom more than ± 0.01 Å (or 0.2%). The corresponding variation in τ is seldom more than ± 50 K (or 2%). In eq 1, the effect of a change in σ is typically 10-fold greater than a change in τ , so the uncertainties in σ and τ arising from scatter in the source data are usually of comparable significance. The derivative $\partial\sigma/\partial T$ is typically about -0.0005 ± 0.0002 Å/K (or 0.01%/K). Although τ is less predictable, even as to the sign of its temperature dependence, $\partial\tau/\partial T$ is in the range 0.3-3 (or $\sim 0.1\%$ /K) for many molecules. The pressure derivative $\partial\sigma/\partial P$ is found both empirically (refractive index data, Figure 8) and theoretically (perturbation theory for LJ fluids, Figure 9) to lie in the range $-0.25 \pm 0.1\%$ /kbar. This is weak enough that it usually does not have a significant effect in fitting the CS-vdW equation to experimental or computer simulation data. Regarding the pressure dependence of τ , we can only infer that it is no more than 1%/kbar, since any larger variation would be expected to produce poor fits to the CS-vdW equation.

As noted in Table III, the quality of the fit obtained is markedly poorer for the haloalkanes, water, and nitrogen. The direction of the deviations is consistent with a decrease in σ with increasing pressure of about the expected sign and magnitude ($\partial\sigma/\partial P \approx -0.1\%$ /kbar). For chloroform, the data⁴⁵ appear suspect. Although the derived σ values are reasonable, the high-pressure densities extrapolate to a value at 1 atm that is 2% higher than a direct measurement; likewise, the high-pressure data give a positive value for $T \partial\tau/\partial T$ whereas a fit using the 1-atm compressibility gives a negative value, as found for similar molecules.

In eq 1, the extremely simple form adopted for the attractive term is surely much less realistic than the repulsive term (CS formula), and this blurs the physical significance of the τ pa-

- (37) Jonas, J.; Hasha, D.; Huang, S. G. *J. Phys. Chem.* **1980**, *84*, 109.
 (38) Jonas, J.; Hasha, D.; Huang, S. G. *J. Chem. Phys.* **1979**, *71*, 3996.
 (39) Dymond, J. H.; Robertson, J.; Isdale, J. D. *Int. J. Thermophys.* **1981**, *2*, 133.
 (40) Dymond, J. H.; Isdale, J. D.; Glen, N. F. *Fluid Phase Equilib.* **1985**, *20*, 305.
 (41) Grindley, T.; Lind, J. E., Jr. *J. Chem. Phys.* **1978**, *68*, 5046.
 (42) *International Critical Tables*; McGraw-Hill: New York, 1928; Vol. III.
 (43) Schroeder, J.; Schlemann, V. H.; Sharo, P. T.; Jonas, J. *J. Chem. Phys.* **1977**, *66*, 3215.
 (44) Campbell, J. H.; Fisher, J. F.; Jonas, J. *J. Chem. Phys.* **1974**, *61*, 346.
 (45) Schroeder, J.; Schlemann, V. H.; Jonas, J. *Mol. Phys.* **1977**, *34*, 1501.
 (46) Van Wijk, W. R.; van der Veen, H. C.; Brinkman, H. C.; Seeder, W. A. *Physica* **1940**, *7*, 44.

- (47) Schindler, W.; Sharko, P. J.; Jonas, J. *J. Chem. Phys.* **1982**, *76*, 3493.
 (48) Fury, M.; Munie, G.; Jonas, J. *J. Chem. Phys.* **1979**, *70*, 1260.
 (49) Parkhurst, H. J.; Jonas, J. *J. Chem. Phys.* **1975**, *63*, 2698.
 (50) Kashiwagi, H.; Fukunaga, T.; Tanaka, Y.; Kubota, H.; Makita, T. *J. Chem. Thermodyn.* **1983**, *15*, 567.
 (51) Levelt, J. M. H. *Physica* **1960**, *26*, 361.
 (52) Michels, A.; Lunbeck, R. J.; Wolkers, G. *J. Physica* **1951**, *9*, 801.

TABLE III: Parameters for CS-vdW Equation and LJ Potential^a

substance	σ	$T \partial\sigma/\partial T$	τ	$T \partial\tau/\partial T$	σ_{LJ}	ϵ_{LJ}/k_B	ref
Alkanes ^b							
<i>n</i> -pentane	5.575	-0.1494	1687	-324	5.49	433	28
isopentane	5.609	-0.1189	1692	-256	5.51	443	28
neopentane	5.501	-0.0823	1482	-515	5.44	380	46
<i>n</i> -hexane	5.959	-0.1124	2017	-549	5.82	517	23
cyclohexane	5.645	-0.1523	2160	-482	5.50	554	37
methylcyclohexane	6.021	-0.1347	2331	-222	5.84	598	38
<i>n</i> -octane	6.550	-0.1057	2407	-574	6.35	617	39
isooctane	6.539	-0.0921	2278	-580	6.35	584	40
<i>n</i> -nonane	6.802	-0.1539	2566	-889	6.58	658	41
<i>n</i> -dodecane	7.529	-0.1883	3171	-1210	7.22	813	39
<i>n</i> -hexadecane	8.313	-0.1127	3775	-1220	7.92	968	23
DEP (C ₉)	6.753	-0.2148	2792	-1030	6.51	716	24
DPH (C ₁₃)	7.682	-0.2098	3350	-1374	7.35	859	24
DBN (C ₁₇)	8.437	-0.1971	3931	-2030	8.03	1008	24
Alcohols							
methanol	3.835	-0.1171	1468	384	3.80	376	22, 42
ethanol	4.435	-0.1290	1673	284	4.37	429	42
1-propanol	4.935	-0.1682	1983	-40.2	4.82	508	42
1-hexanol	6.105	-0.1298	2699	-110	5.89	692	28
ethylene glycol	4.621	-0.1755	2567	-66.5	4.47	658	28
glycerol	5.200	-0.1221	3480	178	4.97	892	28
Haloalkanes ^c							
ethyl chloride	4.674	-0.0960	1482	160	4.63	380	42
ethyl bromide	4.848	-0.1646	1755	-322	4.76	450	42
ethyl iodide	5.028	-0.1235	1891	125	4.92	485	42
<i>n</i> -propyl chloride	5.133	-0.1135	1770	-260	5.04	454	28
<i>n</i> -propyl bromide	5.269	-0.1085	1941	-156	5.15	498	28
<i>n</i> -butyl chloride	5.534	-0.1392	2013	-309	5.40	516	28
<i>n</i> -butyl bromide	5.634	-0.1036	2126	-207	5.49	545	28
<i>n</i> -propyl iodide	5.747	-0.1383	2225	-460	5.59	570	28
<i>n</i> -butyl iodide	5.807	-0.1030	2312	-132	5.64	593	28
Other Liquids							
water ^f	2.922	-0.0136	1445	1270	2.89	371	28
mercury	3.058	-0.1022	3940	1560	2.91	1010	28
CH ₃ CN	4.244	-0.1865	1580	-90.4	4.19	405	43
CS ₂	4.519	-0.1520	1760	-62.6	4.44	451	42
CH ₃ I	4.593	-0.1562	1822	-139	4.50	467	44
CHCl ₃ ^c	5.045	-0.0303	1925	456	4.94	494	45
CCl ₄	5.394	-0.1145	2029	-214	5.26	520	46
acetone	4.850	-0.1859	1822	-453	4.76	467	47
pyridine	5.169	-0.1775	2341	-446	5.02	600	48
benzene	5.292	-0.1792	2172	-625	5.15	557	49, 50
chlorobenzene	5.629	-0.1946	2506	-583	5.45	643	50
bromobenzene	5.735	-0.2019	2705	-689	5.53	694	28
tetramethylsilane	5.913	-0.1421	1713	-355	5.81	439	49
tetraethylsilane	6.965	-0.1443	2721	-830	6.72	698	24
TBA/TBB ^d	8.399	-0.1205	4827	-1160	7.93	1238	24
Supercritical Fluids							
neon	2.524	-0.1288	144	16.5	2.85	37	28
argon	3.242	-0.0874	455	35.6	3.41	117	51
krypton	3.523	-0.1196	626	58.6	3.64	161	28
xenon	3.927	-0.2127	916	-59.6	3.98	235	28
N ₂ ^c	3.451	-0.1609	374	-20.6	3.67	96	28, 52
CO	3.472	-0.1971	381	-40.2	3.69	98	28
CO ₂	3.648	-0.2225	964	-318	3.69	247	28
methane	3.585	-0.2591	552	-70.3	3.73	142	28
ethane	4.240	-0.2845	951	-247	4.29	244	28
propane	4.773	-0.3667	1233	-471	4.76	316	28
butane	5.249	-0.3668	1586	-765	5.18	407	28
ethylene	4.076	-0.1803	899	-107	4.13	230	28
propene	4.639	-0.1810	1260	-275	4.63	323	28

^aQuantities σ and τ and their temperature derivatives evaluated at 20 °C. Units for columns involving σ are Å and for other columns, K. Insignificant digits are retained to avoid round-off errors. ^bLast three entries are symmetric "star" alkanes: 3,3-diethylpentane (DEP), 4,4-dipentylheptane (DHP), and 5,5-dibutylnonane (DBN). ^cFor these substances the fit to eq 1 is markedly poorer than for others, as specified in text, section VA. ^dTetrabutylammonium/tetrabutylborate, a molten organic salt. Data used pertain to $T = 120\text{--}160$ °C and $P = 1\text{--}5000$ atm. The two ions were treated as equivalent moieties with the same σ and τ values.

parameter. For a given substance the nominal τ value generally varies by the order of 10% over the entire liquid and dense fluid regime, and it is not clear how this variation should best be modeled. For convenience, we have chosen to neglect any density dependence of τ . Fortunately, since our chief interest is in the

effective diameter, at high densities where repulsion is dominant even a rather crude allowance for the attractive contribution is useful. There the attractive term becomes almost an additive, pressure-independent constant. For liquids near atmospheric pressure, however, the compressibility is sufficiently large that

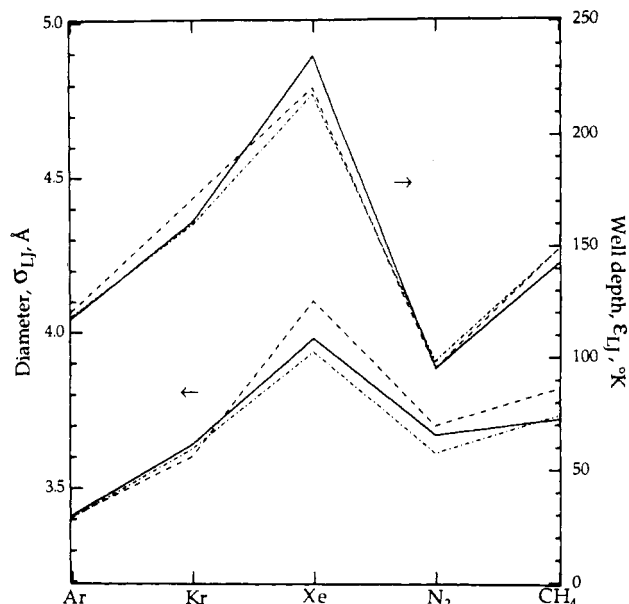


Figure 11. Comparison of Lennard-Jones parameters estimated as described in text (full lines) with results derived from second virial coefficient¹³ (dot-dashed lines) and from application of WCA perturbation theory to equation-of-state data (dashed lines, results of Verlet-Weiss⁵⁴).

the attractive term becomes appreciable. The variation in τ is much larger over the vapor/liquid regime and offers evidence that there it is dominated by density rather than temperature.¹⁶ A more comprehensive form for the attractive contribution might be obtained by exploiting the empirical linearity of the "Zeno line", a locus in the density-temperature plane along which the compressibility factor $Z = P/\rho k_B T$ is unity.⁵³

B. Estimating $\sigma(T,P)$ and LJ Parameters. As emphasized in Figure 10, there are many ways to evaluate σ and τ for the CS-vdW equation when pressure-density isotherms are sparse or lacking. This extends our ability to estimate effective diameters to a wide range of substances with minimal input data. Figure 2 illustrates a striking general result we have confirmed for many examples. The fluid pressure-density isotherms in the high-pressure domain (typically up to ~ 10 kbar) can be predicted quite well, within about 1% for the density, by using values of σ and τ determined solely from data pertaining to atmospheric pressure. For this purpose, we may use either (i) the density ρ_0 and compressibility $\beta = -(1/V)(\partial V/\partial P)_T$ or (ii) the density ρ_0 and the boiling temperature T_b . When the density datum is missing, a good estimate for σ can be obtained just from the molecular structure, which suffices to evaluate the volume V_s from the increments tabulated by Bondi.¹²

The temperature dependence of σ and τ can likewise be determined from data at atmospheric pressure, using (iii) values of ρ_0 and β at two temperatures. For the pressure dependence, very little pertinent experimental data are available, so typically recourse must be had to estimates by analogy or to theory, as illustrated in Figures 8 and 9.

Usually the aim is to estimate thermodynamic or transport properties, and often the requisite diameter corresponds to one of the perturbation theories considered in Figures 6 and 7 or kindred treatments. These typically call for knowledge of the Lennard-Jones potential parameters, σ_{LJ} and ϵ_{LJ} , as in Table II. Since LJ parameters are often lacking or of dubious quality, however, it is useful to exploit the link to the CS-vdW equation as a way to estimate them from more widely accessible quantities. Table III includes the LJ parameters derived from the σ and τ parameters via eqs 3 and 4, using the values of σ_0^* and T_0^* given in Table II for the Monte Carlo data. These are of course nominal estimates, blurred by the noise in the original simulation data (cf. Figure 7). Yet, wherever comparisons can be made, we find rather

good agreement with LJ parameters obtained in the usual way from second virial coefficients¹³ or from much more elaborate analysis of equation-of-state data.⁵⁴ Figure 11 displays such a comparison.

Invoking this link between the CS-vdW and LJ parameters is only justified to the extent that the LJ potential is realistic. Thus, our nominal values of σ_{LJ} and ϵ_{LJ} for complex molecules such as the long-chain alkanes or the strongly associated alcohols are merely empirical or "effective" parameters. These may nonetheless prove useful in estimating other properties. Customary means such as second virial coefficients or vapor viscosity appear unsuitable for estimating such effective LJ parameters for complex molecules; the few available results¹³ exhibit erratic scatter that obscures expected trends, such as an increase in σ_{LJ} and ϵ_{LJ} with increasing chain length in the *n*-alkane series. As seen in Table III, the LJ parameters derived from the CS-vdW equation do show smooth and plausible trends with increasing chain length or chemical properties such as association strength of alcohols. In any case, the link to the empirical correlations of Table I allows easy estimates of LJ parameters. If more incisive data are lacking, we may use eq 4 to estimate the nominal well depth from the boiling temperature via $\epsilon_{LJ}/k_B = 1.72(T_b - 39)$. Likewise, we can evaluate the LJ diameter from eq 3 using our value for ϵ_{LJ} and an estimate of σ , derived if need be merely from the density at 1 atm or from adding up the contributions to V_s , the space-filling volume¹² defined just by the molecular structure. Typically, even with such rudimentary input, the result for ϵ_{LJ} can be expected to agree with other estimates within 10–20% and that for σ_{LJ} within ~ 1 –2%.

C. Applications to Pressure-Dependent Chemistry. Since packing forces dominate many properties of liquids and dense fluids, the corresponding effective diameters are the major ingredient in perturbation theories.^{2–5} Furthermore, in order to relate experimental measurements made at high pressures to theoretical treatments, we must be able to interconvert the pressure and density scales. This requires a good approximation to the equation of state. Thus, there is wide scope for applications of empirical and semitheoretical correlations akin to our Figure 10.

A prototype application is the analysis of pressure-induced vibrational frequency shifts of molecules in solution. Early work by Drickamer and his students⁵⁵ demonstrated the competition between repulsive and attractive forces, manifest in spectral shifts to higher or lower frequency, respectively. In seeking to develop studies of such shifts as a means to evaluate molecular interactions in solution, we found that for certain stretching vibrations the pressure dependence was governed chiefly by the effective hard-sphere diameter of the solvent. For instance, pressure derivatives for the fundamental and first two overtone transitions of iodine in methylcyclohexane solutions were found to agree closely with predictions of a hard-sphere model.⁵⁶ Similar results for the C–C breathing mode of pyridine and benzene in various solvents indicated the feasibility of inverting the data to evaluate the effective solvent diameter.⁵⁷ In pursuing equations of state for these systems, we were led to examine the applicability of eq 1 and found that it provided a simpler and more direct means to determine the effective diameter.

Many other properties of molecular fluids can be predicted once the effective diameter and attractive energy density parameters are determined. These include for instance vibrational dephasing times,⁵⁸ rotational diffusion coefficients,⁵⁹ isotope effects on vapor pressure,⁶⁰ conformational equilibria,⁶¹ and electronic spectral

(54) Verlet, L.; Weis, J.-J. *Mol. Phys.* **1972**, *24*, 1013.

(55) Fishman, E.; Drickamer, H. G. *J. Chem. Phys.* **1956**, *24*, 548. Benson, A. M.; Drickamer, H. G. *J. Chem. Phys.* **1957**, *27*, 1164.

(56) Ben-Amotz, D.; Zakin, M. R.; King, H. E., Jr.; Herschbach, D. R. *J. Phys. Chem.* **1988**, *92*, 1392.

(57) Zakin, M. R.; Herschbach, D. R. *J. Chem. Phys.* **1986**, *85*, 2376; **1988**, *89*, 2380, and work cited therein.

(58) Schweizer, K. S.; Chandler, D. *J. Chem. Phys.* **1982**, *76*, 2296.

(59) Dote, J. L.; Kivelson, D.; Schwartz, R. N. *J. Phys. Chem.* **1981**, *85*, 2169.

(60) Bigeleisen, J.; Lee, M. W.; Mandel, F. *Acc. Chem. Res.* **1975**, *8*, 179.

(61) Pratt, L. R.; Hsu, C. S.; Chandler, D. *J. Chem. Phys.* **1978**, *68*, 4202.

(53) Ben-Amotz, D.; Herschbach, D. R. *Isr. J. Chem.*, in press.

shifts.⁶² In effect, the perturbation methods link all these properties to the equation of state via the σ and τ parameters.

The practical utility of the CS-vdW equation in predicting the density and compressibility of liquids at high pressure deserves emphasis. In that domain, accurate direct measurements become extremely difficult. The ability to predict the pressure-density isotherm at high density by using only input from atmospheric pressure data is thus very welcome. Equation 1 yields an explicit formula for the reciprocal of the compressibility

$$1/\beta = -\rho k_B T [Z + \rho \partial Z / \partial \rho]_T \quad (6)$$

$$= -\rho k_B T [(1 + 4\eta + 4\eta^2 - 4\eta^3 + \eta^4)(1 - \eta)^{-4} - 8(\tau/T)\eta]$$

where in the second line the density dependence of σ and τ is neglected. For example, bromobenzene at 50 °C and atmospheric pressure has $\rho_0 = 1.454 \text{ g/cm}^3$ and $\beta_0 = 0.0776 \text{ kbar}^{-1}$; with these data we find from eqs 1 and 6 values of $\sigma = 5.706 \text{ \AA}$ and $\tau = 2608 \text{ K}$ at 50 °C. With these parameters, the predicted density and compressibility at $P = 7 \text{ kbar}$ are 1.759 g/cm^3 and 0.0122 kbar^{-1} . The predicted density is within 0.1% of the experimental value.²⁸ Although compressibility measurements in this pressure range are not available, the predicted pressure-density isotherm virtually coincides with the experimental points over the full $P = 1 \text{ bar}$ to 7 kbar range. In similar calculations for other substances, including alkanes and alcohols, we find that such predictions of the density match experimental data within better than 1% over the entire high-pressure liquid regime (cf. Figure 2). This consistency indicates that these predictions can be relied on at high pressures for many liquids for which only data at atmospheric pressure are available.

Even when ρ and β are entirely unknown, the high-pressure density can be estimated with fair accuracy by using the empirical correlations of Table I with the molecular structure and boiling temperature. For example, for isooctane the Bondi volume increments predict that $\sigma = 6.58 \text{ \AA}$ at 20 °C. From $T_b = 372 \text{ K}$ we obtain $\tau = 2230 \text{ K}$. These values are quite close to those in Table III fit to high-pressure data (for σ within 0.6%, for τ within 2.0%). The predicted density is 0.672 g/cm^3 at 1 bar and 0.849 g/cm^3 at 5.4 kbar, whereas the experimental values⁴⁰ at 25 °C for these pressures are 0.688 and 0.867 g/cm^3 , respectively, only about 2% higher. As a variant, we can estimate an unknown β or T_b from the molecular structure and density. For instance, for isooctane this route predicts $\beta = -0.129 \text{ kbar}^{-1}$ at 25 °C and $T_b = 395 \text{ K}$, both within about 10%. Several other occasionally useful options for estimating parameters are implicit in Figure 10.

A general theme exemplified by the connections examined in this study is the generic character acquired by dense fluids and liquids at high pressure. This evidently underlies the broad scope and efficacy of such simple correlations and approximations. In Figure 10 the horizontal links, to perturbation theories and molecular dynamics simulations, presume the Lennard-Jones potential. Results obtained from these links thus must reflect the extent to which the LJ form resembles the molecular potential, as well as the adequacy of the CS-vdW equation of state. Which aspect might best repay efforts to introduce more realistic functions remains an open question. The vertical links, to thermodynamic data and other experimental properties, do not involve assumptions about the potential but are subject to the imprecision of empirical correlations. Despite such limitations, it is gratifying to find the high-pressure domain so congenial to transparent approximations for dense fluids.

Acknowledgment. We are much indebted to Harry Drickamer for his generous encouragement, his provocative insights, and many enticing vistas opened up by his classic studies of chemistry at high pressures. This paper is a response to Harry's yearning for pragmatic, "user-friendly" results (and his devotion to baseball). We are also grateful to Jiasai Xu for instructive discussions and especially to Prof. Ernest Grunwald of Brandeis University for

pointing out the utility of molar refraction data for estimating $\partial\sigma/\partial P$.

Appendix A: Boltzmann's Criterion for the Effective Diameter

In 1890 Boltzmann, in discussing collisions of molecules subject to a soft repulsive potential, suggested that the effective hard-sphere diameter σ could be approximated by the distance of closest approach of a colliding pair with the average relative kinetic energy.³⁰ For a central force potential $V(r)$, this corresponds to the criterion $f k_B T = V(\sigma)$, where the factor f is determined by a suitable thermal average of the kinetic energy.^{31,32} This appealing criterion, although not rigorous, was recently found to give good results for diffusion coefficients over a wide range of density and temperature.³² It is readily evaluated for the WCA-LJ core potential

$$V(r) = 4\epsilon_{LJ}(x^2 - x) + \epsilon_{LJ} \quad (A1)$$

where $x = (r/\sigma_{LJ})^{-6}$ and the potential is nonzero only for $r < 2^{1/6}\sigma_{LJ}$. The additive term ϵ_{LJ} serves to shift the effective zero for the kinetic energy to the potential minimum. In reduced units the criterion becomes

$$x^2 - x - 1/4(fT^* - 1) = 0 \quad (A2)$$

This gives eq 3 of the text

$$\sigma(T) = \sigma_0 [1 + (T/T_0)^{1/2}]^{-1/6} \quad (A3)$$

with $\sigma_0 = 2^{1/6}\sigma_{LJ}$ and $T_0 = \epsilon_{LJ}/fk_B$ (or $T_0^* = 1/f$). For a dense fluid it is not apparent what the value of f should be. Andrews³¹ used $f = 3/2$ and Speedy³² used $f = 2$, but we take both σ_0 and T_0 as adjustable parameters in fitting the results of various perturbation theories or molecular dynamics simulations.

Table II lists values of the parameters (in reduced units) obtained from least-squares analysis. The effective diameter does not depend on density for the BH model but does for the WCA and Lado models. We find that for all these variants the σ_0^* parameters are independent of density and have nearly the same value, within 1% of the value $2^{1/6} = 1.1225$ predicted by the simplistic Boltzmann model. The values of T_0^* differ substantially, however. For the WCA and Lado models, we have for convenience simply fit the quantity $(T_0^*)^{-1/2}$ to a cubic polynomial in the reduced density, $\rho^* = \rho\sigma_{LJ}^3$. These fits of eq A3 to the perturbation theories are quite satisfactory. The deviation in $\sigma^*(T)$ is less than $\pm 0.02\%$ for the BH model. The deviation is within $\pm 0.05\%$ for WCA and $\pm 0.03\%$ for Lado, when $0.2 < \rho^* < 0.9$, but increases to about $\pm 0.1\%$ at $\rho^* = 1.1$, the upper end of the range. For the molecular dynamics data, the scatter is appreciable ($\sim 2\%$, as seen in Figure 7), so the fit to eq A3 is less well-determined. For the best fit (dashed curve in Figure 7), the value of σ_0^* is only about 3% higher than for the Boltzmann-Speedy model and the value of T_0^* about 5% higher.

The extremely simple analytic approximation of eq A3 offers a substantial improvement over previous means of evaluating the effective diameters for the perturbation theories. For the WCA model, the standard Verlet-Weis procedure³⁶ requires starting with a value for the BH diameter and iterating to converge to the WCA diameter. Analytical approximations for the BH diameter are already available (with two different choices for the zero of energy),^{21,36} but not for the WCA or Lado models. The simplicity and accuracy of eq A3 make it useful for any calculations involving perturbation theory for Lennard-Jones systems. The Boltzmann criterion can readily be evaluated for other interaction potentials to obtain analogous approximations for the corresponding perturbation theory diameters.

Appendix B: Temperature-Dependent Attractive Energy Density

In the CS-vdW expression for the compressibility factor, eq 1, we introduce in the attractive term a temperature dependence of the form

$$\tau = \tau_0 [1 + (T_A/T)] \quad (B1)$$

(62) Dobrosavljevic, V.; Henebry, C. W.; Stratt, R. M. *J. Chem. Phys.* **1988**, *88*, 5781.

where τ_0 and T_A are constants. This is eq 5 of the text and corresponds to the leading portion of a $1/T$ perturbation expansion, treated by Zwanzig.¹ The τ_0 parameter is positive and T_A usually is also, since experimental results show that τ typically decreases with temperature (although exceptions are not rare, as seen in Table III). The constants may be related to the Boyle temperature T_B , at which the second virial coefficient B_2 vanishes. Since B_2 is proportional to $(1 - \tau/T)$, we have

$$x^2 - x - (T_A/\tau_0) = 0 \quad (\text{B2})$$

with $x = T_B/\tau_0$; hence

$$x = \frac{1}{2}\{1 + [1 - 4(T_A/\tau_0)]^{1/2}\} \quad (\text{B3})$$

When the temperature dependence of τ is weak enough to neglect, $\tau \approx \tau_0$ becomes approximately equal to the Boyle temperature.

Appendix C: Coefficients for Temperature Dependence

Table III tabulates the quantities $T \partial\sigma/\partial T$ and $T \partial\tau/\partial T$. From these the coefficients (σ_0, T_0) and (τ_0, T_A) which occur in eqs 3

and 5 may be obtained by using

$$-T \partial\sigma/\partial T = (\sigma_0/12)[\sigma(T)/\sigma_0]^7(T/T_0)^{1/2} \quad (\text{C1})$$

and

$$-T \partial\tau/\partial T = \tau_0(T_A/T) \quad (\text{C2})$$

with everything evaluated at the reference temperature (20 °C). This yields

$$\sigma_0 = \sigma^{7/6}[\sigma + 12T \partial\sigma/\partial T]^{-1/6} \quad (\text{C3})$$

$$T_0 = T[\sigma + 12T \partial\sigma/\partial T]/[12T \partial\sigma/\partial T]^2 \quad (\text{C4})$$

$$\tau_0 = \tau + T \partial\tau/\partial T \quad (\text{C5})$$

$$T_A = T[-T \partial\tau/\partial T]/[\tau + T \partial\tau/\partial T] \quad (\text{C6})$$

Note that Table III retains insignificant figures in order to avoid round-off error in such calculations.

Frequency Response Analysis of Surface Reactions in Flow Systems

J. R. Schrieffer[†] and J. H. Sinfelt*

Corporate Research Science Laboratories, Exxon Research and Engineering Company, Annandale, New Jersey 08801 (Received: April 28, 1989)

A frequency response analysis is presented for two examples of surface processes occurring in flow systems. The first is concerned with the adsorption and desorption of a simple gas. The second involves a two-step catalytic sequence in which an adsorption-desorption step is followed by a reaction step. Both examples illustrate the utility of frequency response data in yielding basic kinetic information beyond that obtainable with a flow system in the conventional steady-state mode of operation.

I. Introduction

Investigations of the kinetics of surface-catalyzed reactions are commonly conducted under steady-state conditions in flow systems. Frequently, the rate data are obtained at low conversion levels to minimize the variation of reactant concentrations throughout the catalyst bed. The term differential reactor is often used in describing a system operated in this manner.

In a typical investigation, one varies the concentration of a reactant in a stream of gas entering the catalyst bed and observes the effect on the rate of reaction. The data are then fitted to a rate equation derived for a postulated sequence of reaction steps. While studies of this kind represent an important part of any catalytic investigation, the amount of information that one can obtain on the rate constants of the various steps involved in a reaction is limited.

In studies of fast chemical reactions in solution, valuable information on rate constants has been obtained with the aid of relaxation methods, in which a system in equilibrium is perturbed slightly by a rapid change in some external parameter which influences the equilibrium.^{1,2} The adjustment of the system to a new equilibrium is followed and characterized by one or more relaxation times. In one version of the method, the external parameter influencing the equilibrium is oscillated at some frequency ω . The response of the system, as indicated by the concentration of a reactant or product, depends on the time required to attain the new equilibrium. If this relaxation time is large compared to the period of the external oscillation, the reaction will not sense the oscillation. No oscillations in concentration are

then observed. At the other extreme, the relaxation time may be so small that the concentration will oscillate in phase with the external oscillation. When the relaxation time is comparable to the period of the external oscillation, the concentration oscillates at the imposed frequency but is out of phase with it. The phase lag provides a measure of the relaxation time, which in turn contains information on rate constants.

Frequency response studies of this type have been utilized very little for kinetic investigations in surface catalysis. An application to chemisorption kinetics has been reported by Naphtali and Polinski.^{3,4} In their investigation the pressure variation induced by a sinusoidal variation of the volume of a closed adsorption system was measured. More recently, similar types of investigations have been reported by others.⁵⁻⁸ Adsorption and desorption rate constants have been reported for the chemisorption of ethylene on zinc oxide⁶ and of hydrogen on a rhodium catalyst.⁸

The application of frequency response methods to surface reactions in flow systems is a natural extension of these investigations. We consider such an application here. The essence of the method is very simple. The concentration of a reactant in a fluid

(1) Eigen, M. *Discuss. Faraday Soc.* **1954**, *17*, 194.

(2) Eigen, M.; de Maeyer, L. In *Technique of Organic Chemistry*. Vol VIII - Part II. *Rates and Mechanisms of Reactions*, 2nd ed.; Weissberger, A., Ed.; Interscience Publishers: London, 1963; pp 895-1054.

(3) Naphtali, L. M.; Polinski, L. M. *J. Phys. Chem.* **1963**, *67*, 369.

(4) Polinski, L. M.; Naphtali, L. M. *Adv. Catal.* **1969**, *19*, 241.

(5) Yasuda, Y. *J. Phys. Chem.* **1976**, *80*, 1867.

(6) Yasuda, Y. *J. Phys. Chem.* **1976**, *80*, 1880.

(7) Goodwin, J. G., Jr.; Sayari, A.; Lester, J. E.; Marcellin, G. *Am. Chem. Soc., Div. Pet. Chem., Prepr.* **1984**, *29*, 690.

(8) Marcellin, G.; Lester, J. E.; Mitchell, S. F. *J. Catal.* **1986**, *102*, 240.

[†] Permanent address: Institute for Theoretical Physics, University of California, Santa Barbara, CA 93106.